

Methyl Pyruvate on Ni(111): Coverage-Dependent Thermal Chemistry

M. Castonguay, J.-R. Roy, S. Lavoie, M.-A. Laliberté, and P. H. McBreen*

Département de chimie, Université Laval, Québec (Qué). Canada, G1K 7P4

Received: January 15, 2004

The dissociative interaction of methyl pyruvate ($\text{CH}_3\text{COCOOCH}_3$) with Ni(111) was studied between 200 and 450 K. This temperature range includes the typical temperatures, 300–320 K, at which the heterogeneous enantioselective hydrogenation of methyl pyruvate to methyl lactate occurs on supported platinum particles. The observed decomposition of such a relatively complex adsorbate is surprisingly simple; the initial decomposition step involves scission of the CC bond between the two carbonyl functions to form surface acetyl and methoxycarbonyl species. These groups, in turn, undergo decarbonylation to co-deposit CO, hydrocarbon species, and atomic hydrogen. RAIRS measurements made during exposure to methyl pyruvate with the sample held at 250 and 300 K were used to probe the evolution of the composition of the adsorbed layer as a function of coverage. The stability of the different intermediates was highly coverage dependent. A brief comparison of data for methyl pyruvate on Pt(111) and Ni(111) reveals a very different decomposition chemistry on the two metals.

Introduction

The chemisorption of α -ketoesters is of specific interest because of their role in one of the best documented examples of efficient heterogeneous asymmetric catalysis.¹ The asymmetric hydrogenation of methyl pyruvate to methyl lactate on alkaloid modified platinum displays ee values of up to 95%.² A previous study by Castonguay et al.³ dealt with the structure of methyl pyruvate associatively adsorbed on Ni(111) in the 105–200 K range, and this paper provides information on the stability of adsorbed methyl pyruvate and its decomposition products over the 200–450 K temperature range. The asymmetric hydrogenation of ethyl and methyl pyruvate to the corresponding lactates on alkaloid-modified oxide-supported Pt catalysts is carried out in the region of 300–320 K.² Hence, the present study provides data on the stability of methyl pyruvate on clean metal surfaces at typical reaction temperatures. Several surface science studies of ethyl pyruvate and methyl pyruvate on Pt(111) have recently appeared in the literature,^{4,5} thereby enabling a comparison to be made between data for Ni(111) and Pt(111) surfaces. This type of comparison is important for an understanding of why the asymmetric hydrogenation reaction is so metal-dependent. Nickel, in contrast to platinum, is inactive for the reaction.⁶ One of the main reasons why surface science data is only now becoming available for pyruvate adsorption, despite the many related publications to be found in the catalysis literature,¹ is the relative complexity of the pyruvate molecules. Although there is extensive literature on the interaction of monofunctional carbonyl compounds, such as aldehydes,⁷ ketones,⁸ and esters,⁹ with metal surfaces, reports of surface science studies of molecules containing two types of carbonyl groups are rare.¹⁰

Studies of the dissociative adsorption of methyl pyruvate is of additional interest since the molecule contains several functional groups making it a potential source for surface intermediates of relevance to oxygenate synthesis reactions.

Herein we show that the COOCH_3 function is transferred to the metal to form surface methoxycarbonyl.¹¹ Alkoxycarbonyl ligands have been the subject of extensive study in relation to homogeneously catalyzed CO insertion steps in oxygenate synthesis,^{12,13} but, to the best of our knowledge, methyl pyruvate is the first reported precursor for surface methoxycarbonyl.¹¹ Methyl pyruvate also contains three nascent CO molecules, and we show that this property results in a novel method to prepare relatively high coverages of coadsorbed CO and hydrocarbon species. The latter procedure gives the surface scientist an additional methodology by which catalytically active surfaces may be mimicked in UHV studies.

Experimental Section

The experiments were performed in a uHV system equipped with a Mattson Galaxy 4020 FTIR spectrometer, a Micromass quadrupole mass spectrometer, and a Physical Electronics 5100 XPS spectrometer. The heating rate was 1 K/s for the TPD experiments. Exposures were made at a background pressure of 1×10^{-8} Torr. The Ni(111) single crystal (Monocrystals Co.) was cleaned by argon ion sputtering (500 eV) at 300 K, H_2 treatment at 900 K, and annealing to 950 K. Methyl pyruvate (Flucka, purum) was purified by repeated freeze–thaw cycles in the gas handling line. The purity of the adsorbate was also verified by taking ex-situ transmission IR and NMR measurements. The infrared reflectance data were obtained at 4 cm^{-1} resolution in several different acquisition modes. Spectra such as those shown in Figures 2–5 were acquired by first adsorbing methyl pyruvate at 105 K, followed by annealing for 5 s to a specific temperature, cooling to 105 K, recording 800 sample scans, and then taking the ratio to 800 background scans of the clean surface at 105 K. Spectra recorded during gas exposure at 1×10^{-8} Torr, such as those shown in Figures 6 and 7, represent 100 sample scans ratioed to 800 background scans of the clean sample held at the same temperature. The spectra shown in Figure 8 were acquired continuously during a 0.025 K/s temperature ramp. The $\nu(\text{CH})$ spectra shown in Figure 3

* Address correspondence to this author. E-mail: peter.mcBreen@chm.ulaval.ca; fax: 418 656 7916.

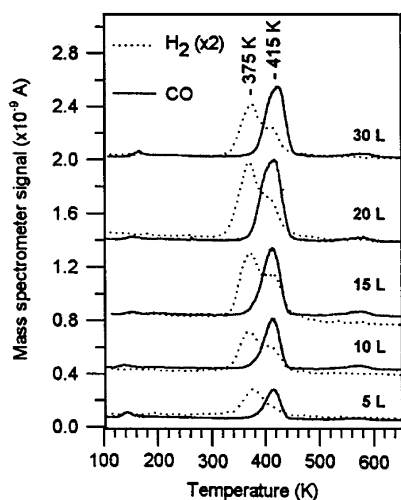


Figure 1. CO and H₂ thermal desorption data for different exposures of methyl pyruvate to Ni(111) at 105 K. An exposure of 20 L at 105 K is sufficient to saturate the monolayer.

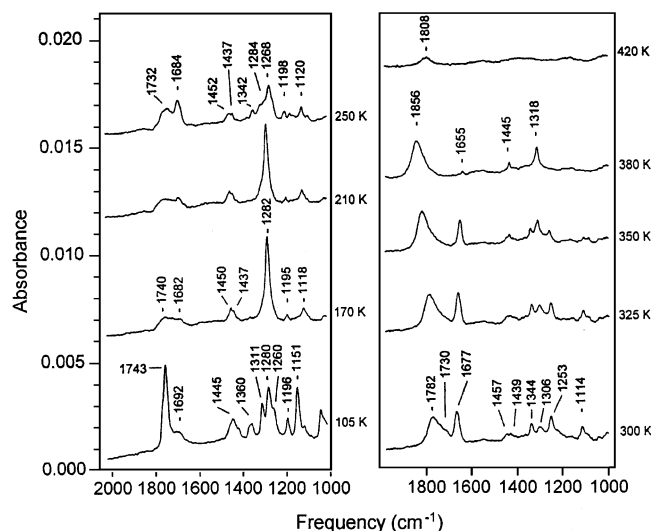


Figure 2. RAIRS spectra recorded for adsorption of methyl pyruvate on Ni(111) at 105 K followed by heating to the indicated temperatures. The initial spectrum, at 105 K, displays bands characteristic of multilayer methyl pyruvate.

were baseline corrected and smoothed with a Savitsky–Golay algorithm, with a great care taken to avoid loss or appearance of features.

Results

A combination of RAIRS and XPS data shows that monolayer completion at 105 K occurs at an exposure of approximately 20 L and that the coverage is linear in exposure. TPD data as a function of exposure are shown in Figure 1. Data for CO and H₂ desorption are plotted together to emphasize the overlap between the two signals. CO desorption occurs at 415 K and desorption maxima for H₂ are observed at 375 and 415 K. Desorption of other products such as methane, ethylene, ethane, or CO₂ was not observed. Desorption from the multilayer occurs at 155 K. XPS analysis at 420 K, following the desorption of hydrogen and carbon monoxide, shows that approximately 25% of the initial monolayer coverage of carbon is left on the surface whereas no oxygen remains. Spectra acquired on annealing multilayer methyl pyruvate on Ni(111) to various temperatures between 105 and 420 K are shown in Figure 2. Annealing from 105 to 170 K removes the multilayer leaving a chemisorbed

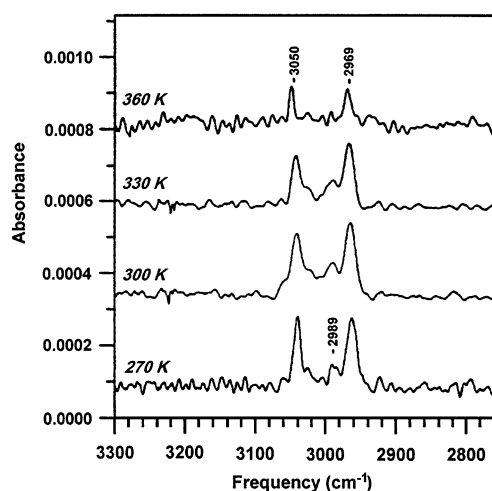


Figure 3. CH stretching region RAIRS spectra for a monolayer of methyl pyruvate on Ni(111) following anneals from 105 K to the indicated temperatures.

layer of *cis*-methyl pyruvate characterized by an intense band at 1282 cm⁻¹ because of the $\nu(\text{C}-\text{O}_\text{e})$, ester group, vibration.^{3,14} Annealing to 250 K leads to the removal of the latter band and its replacement by one of medium intensity at 1268 cm⁻¹. A comparison of the spectra taken on annealing to 210, 250, and 300 K shows that new peaks at ~1677 and 1342 cm⁻¹ begin to grow in at 250 K. Annealing to 300 K leads to an additional carbonyl peak, at 1762 cm⁻¹, because of CO_{ads}. Detailed measurements as a function of annealing temperature reveal that the latter band first appears, at ~1754 cm⁻¹, at 260 K. A subset of the latter measurements, presented as Supplementary Information, reveal the presence, at 270 K, of carbonyl bands at 1776, 1722, and 1686 cm⁻¹, as well as bands at 1453, 1445, 1347, 1255, and 1124 cm⁻¹. (There are small variations in the observed frequencies, for a given temperature or coverage, depending on factors such as dosing conditions, and rate of annealing.) Returning to the data shown in Figure 2, the 300 K spectrum displays carbonyl bands at 1762, 1730–1720, and 1677 cm⁻¹, in addition to bands at 1457, 1439, 1344, 1306, 1253, and 1114 cm⁻¹. Only three bands remain in this region on annealing to 380 K; a band due to CO_{ads} at 1856 cm⁻¹, and bands at 1445 and 1318 cm⁻¹ because of a hydrocarbon deposit. All three bands are removed on heating above 420 K, consistent with the H₂ and CO desorption peaks in Figure 1. The sharp band at ~1677 cm⁻¹ is removed on annealing to above 360 K, coincident with the removal of bands at 1457, 1344, and 1253 cm⁻¹. The band at ~1114 cm⁻¹ is removed between 325 and 350 K. Corresponding spectra for the CH stretching region are shown in Figure 3. Annealing to above 250 K yields sharp peaks at 3050 and 2969 cm⁻¹ and a weak band at 2989 cm⁻¹. The former two bands are attenuated at 360 K while the band at 2989 cm⁻¹ is removed below 360 K.

The RAIRS data presented in Figures 4 and 5 may be used to summarize some of the coverage-dependent complexities of the vibrational spectra of molecularly adsorbed methyl pyruvate on Ni(111). Figures 4 and 5 may also be used as an introduction to the coverage dependence of the decomposition processes. Spectra 4a and 5a are for half- and full-monolayer coverage of molecularly adsorbed methyl pyruvate, respectively. Both spectra are characterized by a complex envelope of carbonyl peaks and a very intense C–O_e stretching band at 1273–1277 cm⁻¹. The half-monolayer spectrum displays a double carbonyl peak, whereas the full monolayer displays a single broad carbonyl peak. When the sample is held at 180–220 K during

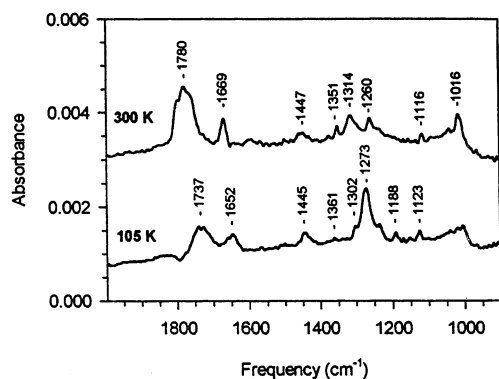


Figure 4. RAIRS spectra for approximately a half a monolayer of methyl pyruvate on Ni(111); (a) at 105 K and (b) following an anneal to 300 K.

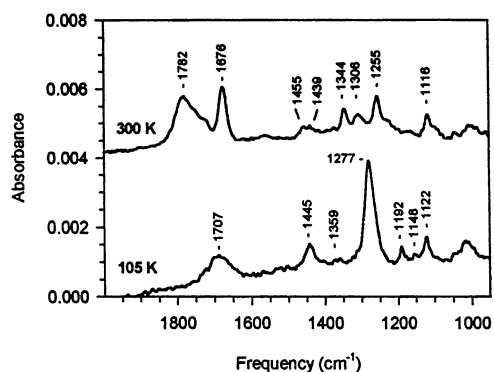


Figure 5. RAIRS spectra for a complete monolayer of methyl pyruvate on Ni(111); (a) at 105 K and (b) following an anneal to 300 K.

exposure, a single broad carbonyl peak is observed at all coverages and is definitively attributed to *cis*-adsorbed methyl pyruvate.³ A more complete description of the results for the associative adsorption of methyl pyruvate on Ni(111) was given in a previous publication.³ Spectra 4b and 5b, obtained on annealing the half- and full-monolayer, respectively, from 105 to 300 K, both show a sharp $\nu(\text{CO})$ band at approximately 1670 cm^{-1} and a broader band, due to CO_{ads} , centered at approximately 1780 cm^{-1} . The spectra obtained on heating to 300 K display two noteworthy differences. First, a band at $\sim 1016 \text{ cm}^{-1}$ is only seen for the half-monolayer experiment. Second, the two carbonyl stretching bands are better resolved in the half-monolayer experiment. In particular, the spectrum for full-monolayer coverage at 300 K (spectrum 5b) displays a shoulder at $\sim 1730 \text{ cm}^{-1}$. The latter shoulder is always accompanied by a band at $\sim 1116 \text{ cm}^{-1}$.

Figures 6 and 7 display RAIRS spectra recorded continuously during exposure at 1×10^{-8} Torr with the sample held at 250 and 300 K, respectively. These spectra permit an overview of the evolution of the adlayer composition as a function of coverage at the two given temperatures. The saturation exposure spectrum in Figure 6 (labeled as 50 L) is essentially identical to the spectrum in Figure 2 for multilayer methyl pyruvate annealed to 250 K. Exposure at 250 K initially leads to a band at 1805 cm^{-1} because of CO_{ads} , a broad feature around 1320 cm^{-1} , and a weak band at 1440 cm^{-1} . As more methyl pyruvate is dosed to the surface, a set of bands at 1744, 1699, 1345, 1294, 1250, and 1122 cm^{-1} grow in simultaneously. Although the saturation spectrum displays frequencies similar to those present in the half-monolayer of molecularly adsorbed pyruvate at 105 K, spectrum 4a, the relative intensities of the bands are very different. Exposure at 300 K leads initially to a CO_{ads} band at 1800 cm^{-1} and features at 1445 and 1311 cm^{-1} . The medium

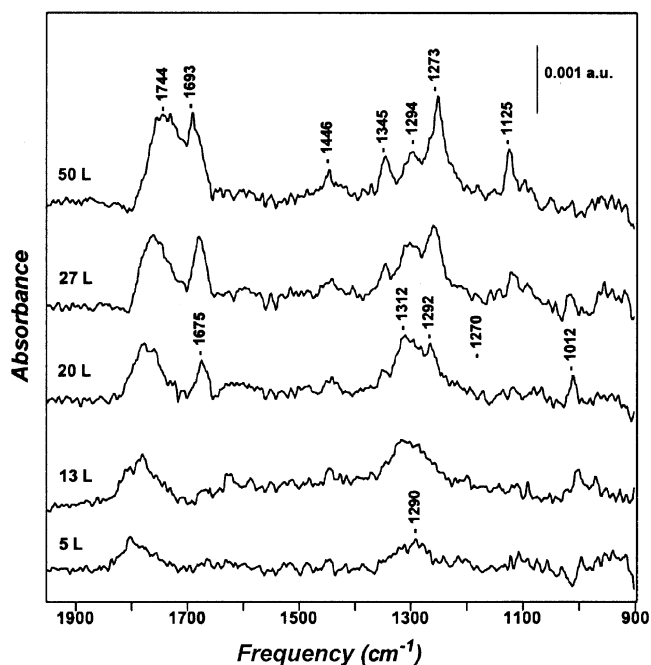


Figure 6. RAIRS spectra acquired during continuous exposure of Ni(111), held at 250 K, to a methyl pyruvate background pressure of 1×10^{-8} Torr.

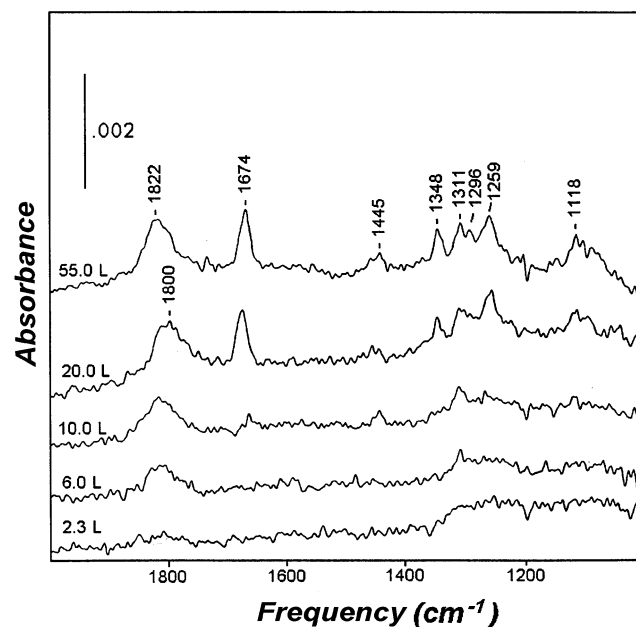
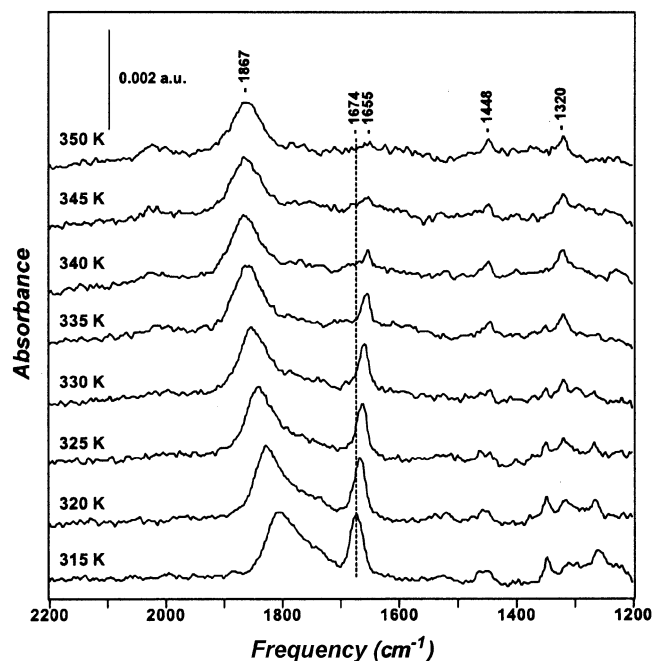


Figure 7. RAIRS spectra acquired during continuous exposure of Ni(111), held at 300 K, to a methyl pyruvate background pressure of 1×10^{-8} Torr.

coverage spectrum (labeled 10 L) in Figure 7 is quite similar to the spectrum in Figure 2 for multilayer methyl pyruvate annealed to 380 K. Saturation exposure is characterized by additional bands at 1674, 1348, 1296, 1259, and 1118 cm^{-1} in common with the 250 K data. The most striking difference between the saturation coverage spectra in Figures 6 and 7 appears in the separation between carbonyl peaks. The 250 K experiment leads to closely spaced peaks at 1744 and 1689 cm^{-1} , while the 300 K experiment yields well-separated peaks at 1822 and 1674 cm^{-1} . In addition, the 250 K saturation coverage spectrum displays a relatively intense peak at 1122 cm^{-1} , compared to the very weak peak observed at 1118 cm^{-1} in the 300 K experiment.

TABLE 1: Comparison of Vibrational Data for Adsorbed Methoxycarbonyl Species Prepared by Annealing Methyl Pyruvate on Ni(111) to 300–325 K with Data for Methyl Pyruvate, Methyl Acetate, and Alkoxy carbonyl Ligands

band frequency (cm ⁻¹)	assignment	frequency data for comparison		
	methoxycarbonyl on Ni(111)	methyl pyruvate ^a	methyl acetate ^b	alkoxy carbonyl ^c
3050	$\nu_a(\text{OCH}_3)$	3035	3028	
2969	$\nu_s(\text{OCH}_3)$	2958	2955	
1677	$\nu(\text{C}=\text{O})$	1737–1762	1747	1650–1680
1457	$\delta_a(\text{OCH}_3)$	1448	1462	
1253	$\nu(\text{C}-\text{OCH}_3)$	1299	1249	

^a Reference 14. ^b Reference 19. ^c Reference 20.**Figure 8.** RARS spectra acquired continuously during an anneal of the methyl pyruvate on Ni(111) system over the temperature 315–350 K temperature range. The initial exposure was performed to multilayer coverage at 105 K. The heating rate was 0.025 K/s.

Additional data from SSIMS (static secondary ion mass spectrometry) measurements, which were discussed in a previous Communication,¹¹ are provided as Supplementary Information. The latter data were recorded during a temperature ramp of Ni(111) dosed to multilayer coverage of methyl pyruvate. Plots of the CH_3CO^- and CH_3O^- signal intensities as a function of temperature show clear changes in slope, toward zero signal, at 328 and 342 K, respectively. RARS data, acquired in an experiment directly analogous to the SSIMS experiment, are presented in Figure 8. The RARS data were obtained continuously during a temperature ramp of Ni(111) dosed, at 105 K, to multilayer coverage. Figure 8 displays, in detail, changes in the carbonyl region that occur in the 315–350 K temperature range. A clear separation between the two carbonyl peaks occurs at approximately 325–330 K. The carbonyl band at 1667 cm⁻¹ is removed on heating to 345–350 K. The latter two changes coincide with the above-mentioned breaks in slope in the SSIMS data.

Discussion

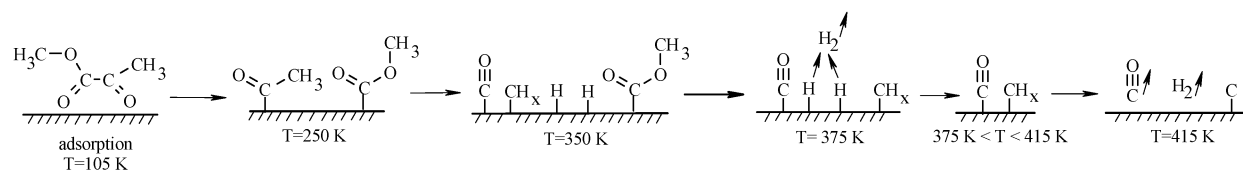
1. Decarbonylation and CC Bond Scission Processes.

Methyl pyruvate contains methyl, methoxy, acetyl, and methoxycarbonyl (COOCH_3) functions as well as three nascent CO molecules. Depending on the coverage and the sample temperature, all of the above species are detected on the surface. The

sequence of RARS spectra in Figure 2 shows the evolution of an intense $\nu(\text{CO})$ band due to CO deposited through the decarbonylation of methyl pyruvate. The band grows in at 260 K (data shown as Supplementary Information) and shifts to higher frequencies in the 1780–1860 cm⁻¹ region as the temperature, and hence the coverage of CO, is increased. This coverage dependence of the $\nu(\text{CO})$ frequency is consistent with well-known dipole–dipole coupling effects.¹⁵ As a point of reference for different aspects of the Discussion given below, we list some observations from the literature on the RARS spectra of CO on clean Ni(111).^{16–18} First, a frequency of 1860 cm⁻¹ for CO on clean Ni(111) is indicative of a coverage of approximately one-third the maximum CO coverage formed under uhv conditions.¹⁷ Second, bands below 1800 cm⁻¹ are only observed at very low coverages of CO on clean Ni(111).¹⁸ Third, a band at 1720 cm⁻¹ is observed for CO on the gently sputtered, and hence defective, Ni(111) surface.¹⁸

The initial decomposition step, prior to any decarbonylation, occurs between 230 and 250 K. This results in the removal of the intense $\nu(\text{C}-\text{O}_e)$ band at 1277 cm⁻¹ and its replacement by a band of medium intensity at 1266 cm⁻¹ (Figure 2). This change is accompanied by the emergence of sharp bands at 1680, 3050, and 2989 cm⁻¹. These four bands are highly characteristic of a species containing a carbonyl group and an OCH_3 group. The comparison to data for methyl pyruvate,^{3,14} methyl acetate,¹⁹ and alkoxy carbonyls²⁰ given in Table 1 permits the four bands to be attributed to surface methoxycarbonyl formed from the COOCH_3 moiety of methyl pyruvate. The bands attributed to methoxycarbonyl are present up to 350–360 K. This rules out any possibility that they are due to a remaining adsorbed state of molecular methyl pyruvate; Figures 4a and 5a and published work³ show that molecularly adsorbed methyl pyruvate on Ni(111) is always characterized by either a broad band or a closely spaced double band in the carbonyl stretching region.³ Two or three features in the RARS spectra that are present in the 250–330 K range cannot be attributed to surface methoxycarbonyl, since they disappear together at temperatures lower than that required to eliminate the methoxycarbonyl bands. As may be seen from Figures 2 and 3, the bands at 1118 and 2989 cm⁻¹ simultaneously disappear while the methoxycarbonyl band at 1684–1662 cm⁻¹ remains relatively intense. We attribute the 1118 and 2989 cm⁻¹ bands to surface acetyl groups, by reference to data for acetyl on Pt(111) surfaces. McCabe et al. attributed a band at 1120 cm⁻¹ to the mixed $\rho(\text{CH}_3) + \nu(\text{CC})$ mode of acetyl on a stepped Pt(111) surface,^{7b} and Zhao et al.^{7c} attributed bands at 2984 and 1122 cm⁻¹ to acetyl on Pt(111). The equivalent bands appear at 2989 and 1096 cm⁻¹ for acetyl prepared by UV irradiation of coadsorbed methyl and CO on supported Rh particles.²¹ The photochemically generated $\text{CH}_3\text{CO}/\text{Rh}/\text{Al}_2\text{O}_3$ system is appropriate for comparison since it represents a

SCHEME 1



crowded surface mixture, containing some of the components present in the adlayer resulting from methyl pyruvate dissociation.

Biacetyl dissociation on Ni(111)²² yields an acetyl peak at $\sim 1666\text{ cm}^{-1}$, and acetyl on stepped Pt(111)^{7c} displays a carbonyl band at 1647 cm^{-1} . These values are typical of both acetyl²³ and alkoxycarbonyl ligands.²⁰ Because of the expected overlap of methoxycarbonyl and acetyl carbonyl bands in the RAIRS spectra, additional measurements were performed using SSIMS.¹¹ The SSIMS data, presented as Supplementary Information, were discussed in a previous Communication.¹¹ The intensities of various secondary ion signals were measured during a temperature ramp of multilayer methyl pyruvate exposed Ni(111). The plot of the CH_3CO^- signal as a function of temperature shows a clear change in slope at 328 K. Similarly, the plot for the OCH_3^- signal displays a change in slope at 345 K. These changes in slope, toward zero signal, are interpreted in terms of the onsets of the sequential removal of acetyl and methoxycarbonyl species at 328 and 345 K, respectively. The onset of removal of the CH_3CO^- signal coincides with the loss (Figure 8) of RAIRS band around 1663 cm^{-1} attributed above to the carbonyl vibration of methoxycarbonyl. The onset of removal of the CH_3CO^- signal coincides with the loss of the weak $\nu(\text{CH})$ band at 2989 cm^{-1} (Figure 3) which was attributed above to acetyl. Indirect support for the presence of an acetyl species is also provided by the spectra shown in Figure 6 for exposure to methyl pyruvate with the sample held at 250 K. The spectrum labeled 13 L displays a broad peak between 1250 and 1350 cm^{-1} and a band at $\sim 1800\text{ cm}^{-1}$. This is consistent with the presence of coadsorbed CH_3 and CO. Methyl groups formed from acetaldehyde decomposition on Ni(111)²² display peaks at 1257 and 1359 cm^{-1} , in good agreement with HREELS data for $\text{CH}_{3\text{ads}}$ on Ni(111).^{24,25} Hence, the CH_3 species are assumed to arise from the decarbonylation of surface acetyl groups. This hydrocarbon deposition gives rise to XPS data showing that 25% of the C(1s) signal due to full-monolayer coverage of methyl pyruvate, at 170 K, remains on the surface at 450 K after CO desorption is complete. We conclude that the RAIRS data provide very strong evidence that the decomposition of methyl pyruvate on Ni(111) leads to the formation of surface methoxycarbonyl and that the combined RAIRS, SSIMS, and XPS data are consistent with the formation of surface acetyl. This conclusion implies that selective CC bond scission occurs, breaking the central CC bond to yield acetyl and methoxycarbonyl.¹¹ Two recent studies, involving biacetyl²² and acetylacetone²⁶ adsorption, provide additional examples of CC bond activation on Ni(111).

The fact that the C–C bond scission is the first reaction that occurs on heating the methyl pyruvate adlayer may be surprising at first because C–H bond activation is usually more facile than C–C bond activation although the C–H bond dissociation energy is greater by about 10 kcal mol^{-1} .²⁷ Taking ethane as an example, CH activation is favored because of the greater number of CH bonds and the hindered accessibility of CC bonds.²⁸ CH activation is also favored by the spherical symmetry of the H 1s orbital in contrast to the sp^3 symmetry at the carbon center. Increasing overlap of metal orbitals with the CC bond

comes at the price of rotation of the two alkyl groups.²⁸ As a result, both experiment^{27,29} and computation^{30,31} show that the C–C bond breaking activation energy is several kcal/mol higher than that for C–H bond breaking. There is very little conjugation between the two carbonyl groups in methyl pyruvate and the central CC bond is a true single bond.³² The organometallic literature on selective CC bond activation^{28,33} suggests several reasons why methyl pyruvate undergoes CC bond scission on Ni(111). First, CC bond activation can be competitive with CH activation in cases where the CC bond is forced into the proximity of the metal through chelation and in the case of coordinative unsaturation of the metal. The Ni(111) surface can fill both conditions for methyl pyruvate. The metal surface is, of course, highly unsaturated. Second, the structural analysis of the RAIRS data shows that methyl pyruvate adsorbs exclusively in the cis-conformation on Ni(111) at 185 K.³ Given that the gas is dosed as a mixture of *cis*- and *trans*-methyl pyruvate, this in turn implies that rotation around the central CC bond (*trans*→*cis* rotamerization) is facile. A transient half-perpendicular/half-parallel geometry with the molecule attached to the surface via one carbonyl oxygen and the other half of the molecule parallel to the surface could readily result in close approach of the CC bond to the surface.¹¹

2. Coverage-Dependent Stability of Surface Intermediates.

The assignment of the RAIRS bands observed at various temperatures leads to the following summary, Scheme 1, of the thermal chemistry of methyl pyruvate on Ni(111).

Scheme 1 is most relevant to experiments involving monolayer or multilayer exposure since, as discussed next, experiments involving submonolayer exposure show that the stability of the decomposition intermediates is highly coverage dependent.

Decarbonylation of methyl pyruvate deposits CO on the surface and it is well known that coadsorbed CO can stabilize hydrocarbon intermediates on surfaces.³⁴ The simplest manifestation of this, in the present study, may be seen in the coverage-dependent thermal desorption data shown in Figure 1. As the coverage of methyl pyruvate, and hence that of deposited CO, is increased, desorption-limited³⁵ removal of CO at 415 K triggers the reaction-limited³⁵ desorption of H_2 at the same temperature. The hydrogen source for the latter desorption is characterized by the bands at 1445 and 1318 cm^{-1} , present at 380 K. This set of bands cannot be assigned readily to any single surface hydrocarbon species on the basis of comparison with data in the literature. In particular, they do not match those observed for CH_3 groups on Ni(111)^{22,24,25} and, in any case, it is highly unlikely that C_1 species are stable on the surface to 360 K.²⁴ In contrast, CC bond containing species are often stable to above room temperature.^{36–39} Furthermore, methyl groups, at high coverages, react to form CC bonds on Pt(111),^{36,37} Mo(100),³⁸ and Ni(100).³⁹ Hence, the two RAIRS bands are tentatively attributed to surface species containing CC bonds produced after the co-deposition of CH_3 and CO from the acetyl moiety of methyl pyruvate.

A second example of the effect of coadsorbed CO is given by the simultaneous disappearance of the $\nu(\text{CO})$ band at 1730 – 1720 cm^{-1} and the bands at 1118 and 2989 cm^{-1} attributed to

surface acetyl. The removal of surface acetyl coincides with the generation of a RAIRS spectrum typical of CO on a clean annealed Ni(111) surface.^{16–18} This coincidence suggests that CO species characterized by the $\nu(\text{CO})$ band at 1730–1720 cm^{-1} serves as a site-blocker to the decarbonylation of surface acetyl. Data taken for full-coverage exposure of methyl pyruvate clearly show the persistence of a carbonyl peak at 1720–1730 cm^{-1} up to approximately 330 K (Figure 8). The band disappears at the same temperature as the bands at 1118 and 2989 cm^{-1} , attributed above to surface acetyl. The band at 1720–1730 cm^{-1} is attributed to an adsorbed state of CO specific to the highly crowded surface. As mentioned above, a band at 1720 cm^{-1} was reported for CO on a nonannealed, gently sputtered, Ni(111) surface.¹⁸ The present studies were carried out on annealed Ni(111). However, the method in which CO is dosed to the surface is vastly different from that for studies on a clean surface. In particular, the decarbonylation process co-doses CO and molecular fragments at temperatures as low as 250 K. Hence, it is possible that a metastable state of adsorbed CO is populated, giving rise to the observed low $\nu(\text{CO})$ stretching frequency. Heating to approximately 325 K removes the latter state, and further annealing to 350 K (Figure 2) leads to CO_{ads} stretching frequencies typical of CO on a clean Ni(111) surface.¹⁶ Zenobi et al.³⁵ have reported measurements consistent with an increased barrier for CO intersite conversion on Ni(111) in the presence of coadsorbed hydrogen. Similarly, strong lateral interactions between adsorbed CO and coadsorbed hydrocarbons have been reported.⁴⁰ Hence, it is not too surprising to see a similar effect in the case of methyl pyruvate decomposition where several species, CO, H, acetyl, CH_3 , and methoxycarbonyl, compete for surface sites.

The thermal stability of surface methoxycarbonyl is also highly dependent on the amount of coadsorbed species. For example, Figure 6 shows that exposure at 250 K initially leads to CO deposition (peak at 1805 cm^{-1}) and hydrocarbon deposition (peak at $\sim 1306 \text{ cm}^{-1}$). Higher exposures lead to the appearance of the methoxycarbonyl $\nu(\text{CO})$ band at 1672 cm^{-1} and a band at 1009 cm^{-1} . A vibrational frequency in the region of 1000 cm^{-1} is immediately suggestive of adsorbed methoxy⁴¹ arising from decarbonylation of methoxycarbonyl. Results for exposure at 300 K (Figure 7) are different in that the methoxycarbonyl features grow in at higher exposures and the methoxy band is not observed. Experiments performed by annealing the half-monolayer and full-monolayer to 300 K also reveal differences. The half-monolayer experiments (Figure 4) lead to a methoxy band at 1016 cm^{-1} whereas the methoxy band is not observed in full monolayer experiments (Figure 5). Overall, the results show that methoxycarbonyl is stable on the crowded surface (Figure 2) to 360 K yet unstable on the mostly clean surface at 250 K (Figure 6). This behavior finds a parallel in that reported in the organometallic literature for alkoxycarbonyl ligands. For example, Bryndza et al.^{20a} reported that bis-methoxycarbonyl complexes are stable to 350 K under normal conditions and to 400 K under 2 atm of CO. The latter conditions are akin to those for high coverages of methyl pyruvate on Ni(111), since an initial high coverage translates into a high coverage of coadsorbed CO at higher temperatures. The extent to which a surface is crowded is obviously an important parameter when comparing surface chemistry with organometallic chemistry.⁴² The stability of methoxycarbonyl in turn determines whether methoxy is observed. If methoxycarbonyl is stable to temperatures above those at which methoxy is stable then the methoxy intermediate will not be detected.

3. Metal Dependence in the Enantioselective Hydrogenation of α -Ketoesters. Surface spectroscopy data on the chemisorption of α -ketoesters have only recently become available in the literature, and it is not surprising that these studies have yielded a complex set of information. NEXAFS and XPS data by Burgi et al.,⁴ for ethyl pyruvate on Pt(111) at 153 K, were interpreted in terms of a chemisorption geometry involving lone pair–metal surface interactions of both carbonyl groups, in agreement with the interpretation given by Castonguay et al.³ for methyl pyruvate on Ni(111). A subsequent in-situ NEXAFS study by Burgi et al. of ethyl pyruvate adsorption on Pt(111) at 298 K in the presence or absence of H_2 ^{4b} was interpreted in terms of a mixture of flat-lying (π -bonded) and lone pair bonded adsorbate, with the flat-lying trans-conformation favored in the presence of coadsorbed hydrogen. Studies by Bonello et al. show that the thermal chemistry of methyl pyruvate on Pt(111) is quite different from that on Ni(111).⁵ The latter authors studied the chemisorption of methyl pyruvate on Pt(111) at 298 K and found convincing STM evidence for an aldol condensation reaction involving the elimination of both a H atom from the keto-methyl group and an OCH_3 group, leading to the formation of a polymer containing up to 40 monomers. They also found that the polymerization reaction could be prevented by the presence of a sufficient coverage of surface hydrogen. Ongoing work in our laboratory on the adsorption of methyl and ethyl pyruvate on Pt(111) provide general support for the interpretation given by Bonello et al. In contrast, the present study of methyl pyruvate on Ni(111) provides no evidence for a polymerization reaction. In particular, the decomposition chemistry differs from that on Pt(111) in that no CO_2 is formed and no high-temperature H_2 desorption tail is observed. In addition, the results for Ni(111) show that the scission of the central CC bond is favored over cleavage of a keto-methyl CH bond. Clearly, the thermal surface chemistry of alkyl pyruvates differs significantly between Pt(111) and Ni(111). This observation implies that the nature of the alkyl pyruvate metal interaction is at least partially responsible for the stringent metal dependence observed for the Orito reaction.

Conclusions

Methyl pyruvate on Ni(111) breaks in two at approximately 250 K to give adsorbed acetyl and methoxycarbonyl species, and both species subsequently undergo decarbonylation leading to high coverages of coadsorbed CO, hydrogen atoms, and hydrocarbon species. RAIRS spectra recorded during exposure to methyl pyruvate with the sample held at 250 and 300 K reveal extensive decomposition at low coverages. These results show that coadsorbed fragments of methyl (or ethyl) pyruvate are likely to be present at the room-temperature conditions appropriate for the enantioselective hydrogenation of α -ketoesters. A comparison to literature data for methyl pyruvate on Pt(111) shows that the decomposition chemistry on Ni(111) is very different from that observed on platinum. This observation suggests that differences in the substrate–metal interaction should be taken into account in attempts to explain the extreme metal sensitivity of the enantioselective hydrogenation reaction.

Acknowledgment. We gratefully acknowledge financial assistance from NSERC (Operating Grant) and FCAR (Équipe et Centre de Recherche (CERPIC)). M.C. and S.L. acknowledge the receipt of NSERC and FCAR graduate scholarships. The machining and electronics support of André Bouffard, André Bilodeau, and Jean Laferrière are gratefully acknowledged.

Supporting Information Available: RAIRS spectra and static secondary ion mass spectrometry data. This material is available free of charge via the Internet at <http://pubs.acs.org>.

References and Notes

- (1) (a) Blaser, H. U.; Jalett, H. P.; Lottenbach, W.; Studer, M. *J. Am. Chem. Soc.* **2000**, *122*, 12675. (b) Baiker, A. *J. Mol. Catal. A: Chem.* **1997**, *115*, 473. (c) Orito, Y.; Imai, S.; Niwa, S. *J. Chem. Soc. Jpn.* **1980**, *4*, 670. (d) Vargas, A.; Burgi, T.; Baiker, A. *J. Catal.* **2001**, *197*, 378. (e) Studer, M.; Blaser, H.-U.; Exner, C. *Adv. Synth. Catal.* **2003**, *345*, 45.
- (2) LeBlond, C.; Wang, J.; Andrews, A. T.; Sun, Y.-K. *J. Am. Chem. Soc.* **1999**, *121*. (b) Zuo, X.; Liu, H.; Liu, M., *Tetrahedron. Lett.* **1998**, *39*, 1941.
- (3) (a) Castonguay, M.; Roy, J.-R.; McBreen, P. *J. Am. Chem. Soc.* **2000**, *122*(3), 518–524. (b) Lavoie, S.; Laliberté, M.-A.; McBreen, P. H. *J. Am. Chem. Soc.* **2003**, *125*, 15756.
- (4) (a) Burgi, T.; Atamny, F.; Schlögl, R.; Baiker, A. *J. Phys. Chem. B* **2000**, *104*, 5953. (b) Burgi, T.; Atamny, F.; Knop-Gericke, A.; Hävecker, M.; Schedel-Niedrig, T.; Schlögl, R.; Baiker, A. *Catal. Lett.* **2000**, *66*, 109. (c) Burgi, T.; Baiker, A. *J. Catal.* **2000**, *194*, 445.
- (5) (a) Bonello, J. M.; Lambert, R. M.; Künzle, N.; Baiker, A. *J. Am. Chem. Soc.* **2000**, *122*, 9864. (b) Bonello, J. M.; Williams, F. J.; Santra, A. S.; Lambert, R. M. *J. Phys. Chem. B* **2000**, *104*, 9696. (c) Bonello, J. M.; Sykes, E. C. H.; Lindsay, R.; Williams, E. J.; Santra, A. K.; Lambert, R. M. *Surf. Sci.* **2001**, *482–485*, 207. (d) Bonello, J. M.; Williams, F. J.; Lambert, R. M. *J. Am. Chem. Soc.* **2003**, *125*, 2723.
- (6) Blaser, H. U.; Jalett, H. P.; Wiehl, Monti, D. M.; Reber, J. F.; Wehrli, Stud. *Surf. Sci. Catal.* **1988**, *41*, 153. (b) Wells, P. B.; Wilkinson, A. G. *Top. Catal.* **1998**, *5*, 39.
- (7) (a) Shekhar, R.; Barteau, M. A.; Plank, R. V.; Vohs, J. M. *J. Phys. Chem. B* **1997**, *101*, 7939–7951. (b) McCabe, R. W.; DiMaggio, C. L.; Madix, R. J. *J. Phys. Chem.* **1985**, *89*, 855. (c) Zhao, H.; Kim, J.; Koel, B. E. *Surf. Sci.* **2003**, *538*, 147.
- (8) Sparks, S. C.; Szabo, A.; Szulczewski, Junker, K.; White, J. M. *J. Phys. Chem. B* **1997**, *101*, 8315.
- (9) Zahidi, E.; Castonguay, M.; McBreen, P. H. *J. Am. Chem. Soc.* **1994**, *116*, 5847.
- (10) Barlow, S. M.; Haq, S.; Raval, R. *Langmuir* **2001**, *17*, 3292.
- (11) Castonguay, M.; Roy, J.-R.; Lavoie, S.; Adnot, A.; McBreen, P. H. *J. Am. Chem. Soc.* **2001**, *123*, 6429.
- (12) (a) Milstein, D.; Huckaby, J. L. *J. Am. Chem. Soc.* **1982**, *104*, 6150. (b) Legrand, C.; Castanet, Y.; Mortreux, A.; Petit, F. *Chem. Commun.* **1994**. (c) Kim, Y.-J.; Osakada, K.; Takenada, A.; Yamamoto, A. *J. Am. Chem. Soc.* **1990**, *112*, 1096. (d) Toth, I.; Elsevier, C. J. *J. Am. Chem. Soc.* **1993**, *115*, 10788. (e) Haynes, A.; Manu, B. E.; Morris, G. E.; Maitlis, P. M. *J. Am. Chem. Soc.* **1993**, *115*, 4093. (f) Chen, C.-C.; Fan, J.-S.; Shieh, S.-J.; Lee, G.-H.; Peng, S.-M.; Wang, S.-L.; Liu, R.-S. *J. Am. Chem. Soc.* **1996**, *118*, 9279.
- (13) (a) Pellegrini, S.; Castanet, Y.; Mortreux, J. *Mol. Catal. A: Chem.* **1999**, *138*, 103. (b) Kapoor, M. P.; Natsumura, Y. *Chem. Commun.* **2000**, 95. (c) De Blasio, N.; Tempesti, E.; Kaddouri, A.; Mazzocchia, G.; Cole-Hamilton, D. J. *J. Catal.* **1998**, *176*, 253.
- (14) (a) Wilmshurst, J. K.; Horwood, J. F. *Aust. J. Chem.* **1971**, *24*, 1183. (b) Dhan, V.; Gupta, R. K. *Indian J. Pure Appl. Phys.* **1996**, *34*, 830.
- (15) Persson, B. N. J.; Ryberg, R. *Phys. Rev. B* **1981**, *24*, 6954.
- (16) Zenobi, R.; Xu, J.; Yates, J. T., Jr. *Surf. Sci.* **1992**, *276*, 241.
- (17) Surnev, L.; Xu, J.; Yates, J. T., Jr. *Surf. Sci.* **1988**, *201*, 1.
- (18) Chen, J. G.; Erley, W.; Ibach, H. *Surf. Sci.* **1989**, *223*, L891.
- (19) Hollenstein, H.; Gunthard, Hs. H. *J. Mol. Spectrosc.* **1980**, *84*, 457.
- (20) (a) Bryndza, H. E.; Kretchmar, S. A.; Tulip, T. H. *J. Chem. Soc., Chem. Commun.* **1985**, 977. (b) Murray, T. F.; Norton, J. R. *J. Am. Chem. Soc.* **1979**, *101*, 4107. (c) Dockter, D. W.; Fanwick, P. E.; Kubiak, C. P. *J. Am. Chem. Soc.* **1996**, *118*, 4846.
- (21) Wong, J. C. S.; Yates, J. T. *J. Phys. Chem.* **1995**, *99*, 12640.
- (22) Roy, J.-R.; Castonguay, M.; Laliberté, M.-A.; McBreen, P. H. submitted for publication.
- (23) McFarlane, K. L.; Lee, B.; Fu, W.; van Eldik, R.; Ford, P. C. *Organometallics* **1998**, *17*, 1826.
- (24) Yang, Q. Y.; Maynard, K. J.; Johnson, A. D.; Ceyer, S. T. *J. Chem. Phys.* **1995**, *102*, 7734.
- (25) Castro, M. E.; Chen, J. G.; Hall, R. B.; Mims, C. A. *J. Phys. Chem. B* **1997**, *101*, 4060.
- (26) Sim, W.-S.; Li, T.-C.; Yang, P.-X.; Yao, B.-S. *J. Am. Chem. Soc.* **2002**, *124*, 4970.
- (27) Johnson, D.; Weinberg, W. H. *J. Chem. Soc., Faraday Trans.* **1995**, *91*, 3695.
- (28) Millstein, D.; Rybtchinski, B. *Angew. Chem., Int. Ed.* **1999**, *38*, 871.
- (29) Schultz, R. H.; Armentrout, P. B. *J. Am. Chem. Soc.* **1991**, *113*, 729.
- (30) Low, J. J.; Goddard, W. A., III. *J. Am. Chem. Soc.* **1984**, *106*, 8321.
- (31) Siegbahn, P. E. M.; Blomberg, M. R. A. *J. Am. Chem. Soc.* **1992**, *114*, 10549.
- (32) Meeks, J. L.; Maria, H. J.; Brint, P.; McGlynn, S. P. *Chem. Rev.* **1975**, *75*, 604.
- (33) (a) Sundermann, A.; Uzan, O.; Milstein, D.; Martin, J. M. L. *J. Am. Chem. Soc.* **2000**, *122*, 7096. (b) Chatani, N.; Ie, Y.; Kakiuchi, F.; Murai, S. *J. Am. Chem. Soc.* **1999**, *121*, 8645. (c) Suggs, J. W.; Jun, C.-H. *J. Chem. Soc. Chem. Commun.* **1985**, 92. (d) Suggs, J. W.; Jun, C.-H. *J. Am. Chem. Soc.* **1984**, *106*, 3054. (e) Edelbach, B. L.; Lachicotte, R. J.; Jones, W. D. *J. Am. Chem. Soc.* **1998**, *120*, 2843. (f) Kondo, T.; Nakamura, A.; Okada, T.; Suzuki, N.; Wada, K.; Mitsudo, T.-A. *J. Am. Chem. Soc.* **2000**, *122*, 6319.
- (34) (a) Hills, M. M.; Parmeter, J. E.; Weinberg, W. H. *J. Am. Chem. Soc.* **1986**, *108*, 7215. (b) Chen, J.-J.; Winograd, N. *Surf. Sci.* **1994**, *314*, 188. (c) Burke, M. L.; Madix, R. J. *J. Am. Chem. Soc.* **1991**, *113*, 1476. (d) Henderson, M. A.; Mitchell, G. E.; White, J. M. *Surf. Sci.* **1991**, *248*, 279. (e) Sasaki, T.; Kawada, F.; Aruga, T.; Iwasawa, Y. *Surf. Sci.* **1992**, *278*, 291.
- (35) Zenobi, R.; Xu, J.; Yates, J. T., Jr. *Surf. Sci.* **1992**, *276*, 241.
- (36) Fairbrother, D. H.; Peng, X. D.; Trenary, M.; Stair, P. C. *J. Chem. Soc., Faraday Trans.* **1995**, *91*, 3619.
- (37) Oakes, D. J.; Newell, H. E.; Rutten, F. J. M.; McCoustra, M. R. S.; Chesters, M. A. *J. Vac. Sci. Technol., A* **1996**, *14*, 1439.
- (38) Kim, S. H.; Stair, P. C. *J. Am. Chem. Soc.* **1998**, *120*, 8535.
- (39) Dickens, K. A.; Stair, P. C. *Langmuir* **1998**, *14*, 1444.
- (40) Rousseau, G. B. D.; Bovet, N.; Johnston, S. M.; Lennon, D.; Dhanak, V.; Kadowala, F. *Surf. Sci.* **2002**, *511*, 190.
- (41) McBreen, P. H.; Erley, W.; Ibach, H. *Surf. Sci.* **1983**, *133*, L649.
- (42) Torkelson, J. R.; Antwi-Nsiah, F. H.; McDonald, R.; Cowie, M.; Pui, J. G.; Jalkanen, K. J.; DeKock, R. L. *J. Am. Chem. Soc.* **1999**, *121*, 3666.